PERGAMON

International Journal of Solids and Structures 38 (2001) 8331–8344

INTERNATIONAL JOURNAL OF SOLIDS and STRUCTURES

www.elsevier.com/locate/ijsolstr

Fracture analysis of piezoelectric materials with defects using energy density theory

Ai Kah Soh [a,*], Dai-Ning Fang [b], Kwok Lun Lee [a]

[a] *Department of Mechanical Engineering, The University of Hong Kong, Pokfulam Road, Hong Kong*
[b] *Department of Engineering Mechanics, Tsinghua University, Beijing 100084, China*

Received 16 August 2000; in revised form 20 March 2001

Abstract

The objective of this paper is to extend a failure criterion, which is based on the energy density factor, for an elliptical cavity or a line crack embedded in an infinite piezoelectric solids, subjected to a combined in-plane electrical and mechanical loading. In the present analysis, the exact electric boundary conditions are applied at the rim of the cavity/crack. This is to avoid the common assumption of impermeable or permeable crack, which does not reflect the practical situation. The direction of crack initiation or subsequent post-failure, and the critical loads for fracture, can be predicted using the total energy density factor, S. This factor is a function of the aspect ratio of the elliptical cavity, the electromechanical loading, core region outside the crack tip, permittivity of vacuum and material constants. The results obtained agree with the experimental observation, i.e. a positive electric field enhances crack growth while a negative electric field impedes crack growth. Moreover, the results indicate that the critical fracture loads are under-estimated by the assumption of impermeable crack and over-estimated when the crack is assumed to be permeable for $E_2^{\text{app}} > 0$, where E_2^{app} is the applied electric field. However, the fracture loads are over-estimated by the assumption of impermeable crack and under-estimated when the crack is assumed to be permeable for $E_2^{\text{app}} < 0$. The energy density criterion has the advantage of possessing the capability to implement the exact electric boundary conditions. This is due to the fact that the criterion can link the behavior of a crack to that of an elliptical cavity by consistent application of this criterion to a thin layer near the cavity/crack boundary. © 2001 Elsevier Science Ltd. All rights reserved.

Keywords: Energy density; Piezoelectric material; Fracture criterion; Energy release rate; Elliptical cavity; Crack

1. Introduction

The fracture problems of piezoelectric materials have received much attention in the last few years. Thus, vast amount of theoretical results have been obtained by many researchers (Parton, 1976; Deeg, 1980; McMeeking, 1989, 1990; Pak, 1990; Sosa and Pak, 1990; Suo et al., 1992; Sosa, 1992; Dunn, 1994; Park

* Corresponding author. Tel.: +852-2859-8061; fax: +852-2858-5415.
E-mail address: aksoh@hkucc.hku.hk (A.K. Soh).

0020-7683/01/$ - see front matter © 2001 Elsevier Science Ltd. All rights reserved.
PII: S0020-7683(01)00080-4

and Sun, 1995; Zhang and Tong, 1996; Gao et al., 1997; and Fang et al., 2000). However, nearly all the previous analyses were based on the assumption of impermeable or permeable crack, i.e., the crack faces were assumed to be impermeable or permeable to electric field and, hence, the electric displacement vanishes or continues inside the crack, respectively. In fact, these two extreme cases are not realistic, e.g., Park and Sun (1995) pointed out that the assumption of impermeable crack contradicts many experimental observations. Since the dielectric constant of the air or vacuum inside the crack is neither zero nor the dielectric permittivity of the material (McMeeking, 1989; Dunn, 1994; Fang and Soh, 2001), the crack problems in a piezoelectric material should be treated as electric inclusion problems. Consequently, Sosa and Khutoryansky (1996) used the series expansion method to address the plane problem of a transversely isotropic piezoelectric medium with an elliptical hole.

Many fracture criteria for piezoelectric materials have been proposed in the recent years, e.g., the total potential (Pak, 1990; Suo et al., 1992), the mechanical (Park and Sun, 1995) and the local (Gao et al., 1997) energy release rates, and the energy criterion considering domain switching dissipation (Fang et al., 2000). Pak (1990) found that the presence of applied electric field always reduced the total potential energy release rate. This implies that a crack is impeded by the electric field regardless of its direction. This conclusion contradicts the existing experimental data. Later, Park and Sun (1995) proposed to use only the mechanical part of the energy as a criterion by arguing that fracture is a mechanical process and, therefore, it should be controlled by the mechanical part of the energy release rate. But, this argument is unsound because there is no fundamental reason to separate a physical process into an electric part and a mechanical part, in view of the fact that all mechanical forces are of electromagnetic origin. As a result, Gao et al. (1997) proposed a criterion based on the local energy release rate of an electrically yielded crack. However, the effect of domain switching cannot be accounted for using this model. In line with Griffith's theory on mechanical fracture, Fang et al. (2000) proposed a criterion based on energy balance with the consideration of domain switching dissipation. However, they only proposed an energy balance approach and the results are the same as those of Gao et al. (1997).

Sih (1991) has proposed a fracture theory based on the field strength of the local strain energy density. This theory requires no calculation of energy release rate and, thus, it possesses the inherent advantage of being able to treat all mixed mode crack extension problems. The stationary value of this density factor can predict the direction of crack growth in any condition. In addition, the critical value S_{cr} has been shown to be independent of the crack geometry and loading and, hence, it can be used as a material parameter for measuring the resistance against fracture. Recently, Shen and Nishioka (2000) used this theory to develop a fracture criterion for piezoelectric materials. Their theoretical result agrees qualitatively with the empirical evidence by assuming impermeable crack.

In the present study, the energy density fracture analysis of an elliptic cavity or a crack, in a transversely isotropic piezoelectric solid subjected to remote loading, is carried out. This study adopts the approach and the assumption of exact electric boundary conditions employed by Sosa and Khutoryansky (1996). First of all, a surface layer criterion (Sih, 1991) is used to locate the position where the fracture of the elliptic cavity is expected to initiate. The direction of crack initiation and subsequent post-failure can be described by the total energy density factor, S, from which the critical loads for fracture can be predicted.

2. Basic equations

Fig. 1 shows an infinite poled piezoelectric ceramic, in which a central elliptic cavity of major and minor semi-axes, a and b, respectively, is embedded. This piezoelectric ceramic plate is subjected to a remote in-

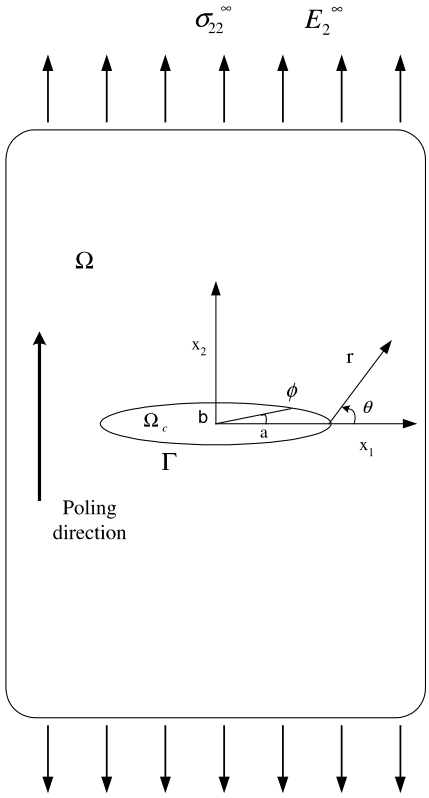

Fig. 1. Schematic diagram of an elliptical cavity embedded in a piezoelectric solid subjected to uniform loading at infinity.

plane electrical loading, E_2^{∞}, and mode I mechanical loading, σ_{22}^{∞}. The cavity is assumed to be filled with a dielectric medium of permittivity, ε_0, and it is free of traction force and charge. The ceramic is poled in the positive direction of the x_2 axis.

The general equations governing the three-dimensional theory of piezoelectricity in the absence of body forces and free charges are as follows:

$$\varepsilon_{ij} = s_{ijkl}\sigma_{kl} + g_{kij}D_k \tag{1a}$$

$$E_i = -g_{ikl}\sigma_{kl} + \beta_{ik}D_k \tag{1b}$$

where $i, j, k, l = 1, 2, 3$; σ_{ij}, D_i, ε_{ij}, E_i are the components of stress, electric displacement, strain and electric field, respectively; and s_{ijkl}, g_{kij} and β_{ik} represent the compliance tensor of material, piezoelectric tensor and dielectric impermeability tensor, respectively.

For a transversely isotropic solid in Cartesian coordinate system x, y, z, assuming that x–y is the isotropic plane and z is the poling direction, the constitutive equations (1a) and (1b) can be written as:

$$\begin{Bmatrix} \varepsilon_{xx} \\ \varepsilon_{yy} \\ \varepsilon_{zz} \\ 2\varepsilon_{zy} \\ 2\varepsilon_{zx} \\ 2\varepsilon_{xy} \end{Bmatrix} = \begin{bmatrix} s_{11} & s_{12} & s_{13} & 0 & 0 & 0 \\ s_{12} & s_{11} & s_{13} & 0 & 0 & 0 \\ s_{13} & s_{13} & s_{33} & 0 & 0 & 0 \\ 0 & 0 & 0 & s_{44} & 0 & 0 \\ 0 & 0 & 0 & 0 & s_{44} & 0 \\ 0 & 0 & 0 & 0 & 0 & 2(s_{11}-s_{12}) \end{bmatrix} \begin{Bmatrix} \sigma_{xx} \\ \sigma_{yy} \\ \sigma_{zz} \\ \sigma_{zy} \\ \sigma_{zx} \\ \sigma_{xy} \end{Bmatrix} + \begin{bmatrix} 0 & 0 & g_{31} \\ 0 & 0 & g_{31} \\ 0 & 0 & g_{33} \\ 0 & g_{15} & 0 \\ g_{15} & 0 & 0 \\ 0 & 0 & 0 \end{bmatrix} \begin{Bmatrix} D_x \\ D_y \\ D_z \end{Bmatrix} \tag{2a}$$

$$\begin{Bmatrix} E_x \\ E_y \\ E_z \end{Bmatrix} = -\begin{pmatrix} 0 & 0 & 0 & 0 & g_{15} & 0 \\ 0 & 0 & 0 & g_{15} & 0 & 0 \\ g_{31} & g_{31} & g_{33} & 0 & 0 & 0 \end{pmatrix} \begin{Bmatrix} \sigma_{xx} \\ \sigma_{yy} \\ \sigma_{zz} \\ \sigma_{zy} \\ \sigma_{zx} \\ \sigma_{xy} \end{Bmatrix} + \begin{pmatrix} \beta_{11} & 0 & 0 \\ 0 & \beta_{11} & 0 \\ 0 & 0 & \beta_{33} \end{pmatrix} \begin{Bmatrix} D_x \\ D_y \\ D_z \end{Bmatrix} \tag{2b}$$

In order to study the electromechanical interaction explicitly, the three-dimensional model is reduced to a two-dimensional one by assuming either x–z or y–z plane as the plane of analysis. For the purpose of convenience, the former, which is the same as that chosen by Sosa (1992), is selected by assuming that

$$\varepsilon_{yy} = \varepsilon_{zy} = \varepsilon_{xy} = E_y = 0 \tag{3}$$

By renaming the index $x \to 1$, $z \to 2$ and minimizing the notation of constants, Eqs. (2a) and (2b) becomes

$$\begin{Bmatrix} \varepsilon_{11} \\ \varepsilon_{22} \\ 2\varepsilon_{12} \end{Bmatrix} = \begin{bmatrix} a_{11} & a_{12} & 0 \\ a_{12} & a_{22} & 0 \\ 0 & 0 & a_{33} \end{bmatrix} \begin{Bmatrix} \sigma_{11} \\ \sigma_{22} \\ \sigma_{12} \end{Bmatrix} + \begin{bmatrix} 0 & b_{21} \\ 0 & b_{22} \\ b_{13} & 0 \end{bmatrix} \begin{Bmatrix} D_1 \\ D_2 \end{Bmatrix} \tag{4a}$$

$$\begin{Bmatrix} E_1 \\ E_2 \end{Bmatrix} = -\begin{bmatrix} 0 & 0 & b_{13} \\ b_{21} & b_{22} & 0 \end{bmatrix} \begin{Bmatrix} \sigma_{11} \\ \sigma_{22} \\ \sigma_{12} \end{Bmatrix} + \begin{bmatrix} c_{11} & 0 \\ 0 & c_{22} \end{bmatrix} \begin{Bmatrix} D_1 \\ D_2 \end{Bmatrix} \tag{4b}$$

where

$$\begin{aligned} &a_{11} = s_{11} - \frac{s_{12}^2}{s_{11}}, \quad a_{12} = s_{13} - \frac{s_{12}s_{13}}{s_{11}}, \quad a_{22} = s_{33} - \frac{s_{13}^2}{s_{11}}, \quad a_{33} = s_{44} \\ &b_{21} = \left(1 - \frac{s_{12}}{s_{11}}\right) g_{31}, \quad b_{22} = g_{33} - \frac{s_{13}}{s_{11}} g_{31}, \quad b_{13} = g_{15}, \quad c_{11} = \beta_{11}, \quad c_{22} = \beta_{33} + \frac{g_{31}^2}{s_{11}} \end{aligned} \tag{5}$$

By adopting Sosa's approach (1992), the field solutions for the two-dimensional problem can be expressed as

$$\boldsymbol{\sigma} = 2\,\mathrm{Re} \sum_{k=1}^{3} \begin{Bmatrix} \mu_k^2 \\ 1 \\ -\mu_k \end{Bmatrix} \varphi_k'; \qquad \boldsymbol{D} = 2\mathrm{Re} \sum_{k=1}^{3} \begin{Bmatrix} \mu_k \\ -1 \end{Bmatrix} \lambda_k \varphi_k'; \qquad \boldsymbol{E} = 2\mathrm{Re} \sum_{k=1}^{3} \begin{Bmatrix} 1 \\ \mu_k \end{Bmatrix} \kappa_k \varphi_k' \tag{6}$$

where Re and Im denote the real and imaginary part, respectively; μ_k are distinct complex parameters to be obtained from the characteristic equation (Sosa, 1992), and φ_k (as functions of three complex variables $z_k = x_1 + \mu_k x_2$) are the three complex potentials to be determined.

The complex potentials are linked to the boundary conditions. Firstly, the problem that we consider is an infinite piezoelectric body containing an elliptic cavity of major and minor axes $2a$ and $2b$, along x_1 and x_2, respectively. The uniform stresses σ_{11}^{∞}, σ_{12}^{∞}, σ_{22}^{∞} and electric displacements D_1^{∞}, D_2^{∞} are applied remotely.

The cavity is assumed to be filled with a homogeneous medium of dielectric permittivity ε_0, and it is free of forces and surface charge density (Sosa and Khutoryansky, 1996).

3. Solution for an elliptic cavity

By applying the procedure proposed by Sosa and Khutoryansky (1996), the field solutions for two-dimensional problems based on the exact electric boundary conditions can be expressed as

$$\boldsymbol{\sigma} = \begin{pmatrix} \sigma_{11} \\ \sigma_{22} \\ \sigma_{12} \end{pmatrix} = \begin{pmatrix} \sigma_{11}^{\infty} \\ \sigma_{22}^{\infty} \\ \sigma_{12}^{\infty} \end{pmatrix} + 2\mathrm{Re}\sum_{k=1}^{3} \begin{Bmatrix} \mu_k^2 \\ 1 \\ -\mu_k \end{Bmatrix} L_k \tag{7}$$

$$\boldsymbol{D} = \begin{pmatrix} D_1 \\ D_2 \end{pmatrix} = \begin{pmatrix} D_1^{\infty} \\ D_2^{\infty} \end{pmatrix} + 2\mathrm{Re}\sum_{k=1}^{3} \begin{Bmatrix} \mu_k \\ -1 \end{Bmatrix} \lambda_k L_k \tag{8}$$

Using the constitutive equation, i.e. Eqs. (4a) and (4b), together with Eqs. (7) and (8), the strain and electric field can be expressed as:

$$\boldsymbol{\varepsilon} = \begin{pmatrix} \varepsilon_{11} \\ \varepsilon_{22} \\ 2\varepsilon_{12} \end{pmatrix} = \begin{pmatrix} \varepsilon_{11}^{\infty} \\ \varepsilon_{22}^{\infty} \\ \varepsilon_{12}^{\infty} \end{pmatrix} + 2\mathrm{Re}\sum_{k=1}^{3} \begin{pmatrix} a_{11}\mu_k^2 + a_{12} - b_{21}\lambda_k \\ a_{12}\mu_k^2 + a_{22} - b_{22}\lambda_k \\ -a_{33}\mu_k + b_{13}\lambda_k\mu_k \end{pmatrix} L_k \tag{9}$$

$$\boldsymbol{E} = \begin{pmatrix} E_1 \\ E_2 \end{pmatrix} = \begin{pmatrix} E_1^{\infty} \\ E_2^{\infty} \end{pmatrix} + 2\mathrm{Re}\sum_{k=1}^{3} \begin{pmatrix} 1 \\ \mu_k \end{pmatrix} \kappa_k L_k \tag{10}$$

where

$$L_k = L_k(\mu_k, z_k) = \frac{-m_{k1}}{\zeta_k^2 w_k'(\zeta_k)} \tag{11}$$

in which ζ_k are the complex coordinates in the mapped plane, $w_k(\zeta_k)$ is the conformal function. Note that m_{k1} in the third expression of Eq. (11) correspond to a_{k1} employed by Sosa and Khutoryansky (1996).

The expressions given in Eqs. (7)–(10) are valid everywhere in Ω. In order to determine the failure location along the boundary of the ellipse, change of variables is introduced as follows:

$$z_k = a\cos\phi + \mu_k b\sin\phi \tag{12}$$

where $-\pi \leqslant \phi < \pi$ is measured along the boundary of the ellipse. Thus, we obtain (Sosa and Khutoryansky, 1996)

$$L_k = L_k(\mu_k, \phi) = \frac{m_{k1}(\sin\phi + \mathrm{i}\cos\phi)}{a\sin\phi - \mu_k b\cos\phi} \tag{13}$$

For an elliptical notch, a surface layer criterion proposed by (Sih, 1991) can be employed as a preliminary judgment to locate the position ϕ, at which fracture may initiate from the notch surface. Note that ϕ denotes the angle between the direction of crack propagation and that of the positive major semi-axis of the elliptical notch, as shown in Fig. 1. Once the angle ϕ is determined, the knowledge of the energy stored in an element outside the core region (near the apex of the elliptical notch) is used as a means for establishing the failure location at some points in the bulk of the solid.

The energy associated with the surface layer can be derived from the mechanics of thin layer. On Γ, the radial stress is equal to zero. Thus, the element in the thin layer is subjected to uniaxial tension. The tangential stress and strain and the electric displacement and field are, respectively, given by

$$\sigma_{ss}(\phi) = \frac{1}{\Theta^2}\left[\sigma_{11}\sin^2\phi - 2\sigma_{12}\alpha\sin\phi\cos\phi + \sigma_{22}\alpha^2\cos^2\phi\right] \tag{14}$$

$$\varepsilon_{ss}(\phi) = \frac{1}{\Theta^2}\left[\varepsilon_{11}\sin^2\phi - 2\varepsilon_{12}\alpha\cos\phi\sin\phi + \varepsilon_{22}\alpha^2\cos^2\phi\right] \tag{15}$$

$$D_s(\phi) = \frac{1}{\Theta}\left[-D_1\sin\phi + D_2\alpha\cos\phi\right] \tag{16}$$

$$E_s(\phi) = \frac{1}{\Theta}\left[-E_1\sin\phi + E_2\alpha\cos\phi\right] \tag{17}$$

where $\Theta = \sqrt{\alpha^2\cos^2\phi + \sin^2\phi}$

Therefore, the strain energy per unit area of the surface layer can be expressed as

$$\gamma_e = (\tfrac{1}{2}\sigma_{ss}\varepsilon_{ss} + \tfrac{1}{2}E_sD_s)\delta \tag{18}$$

where δ is a parameter for quantifying the surface condition. Note that $\gamma_e/\delta\sigma^2\pi a$ is a convenient non-dimensional form for indicating strain energy. A notched specimen may be loaded to failure and the strain energy per unit surface layer can be computed from Eq. (18). The location of initial failure (i.e., the angle of crack propagation, ϕ) on the notch boundary is then determined by setting $\partial\gamma_e/\partial\phi = 0$ for γ_e to reach its maximum value.

4. Solution for a crack

The field solutions for a crack are similar to those for an elliptical cavity by taking the former as the limiting case of the latter, i.e., let $b \to 0$. One of the objectives of this study is to predict the direction of crack propagation for both an elliptical cavity and a line crack, which in turn, gives the distributions of the electromechanical fields in the vicinity of the crack tip. This is achieved by assuming that

$$z_k = a + r\cos\theta + \mu_k r\sin\theta \tag{19}$$

where $r > 0$, $-\pi \leqslant \theta \leqslant \pi$ and $r/a \leqslant 1$. Note from Fig. 1 that the original coordinates for the crack tip are different from those for the elliptical cavity. Hence, the third expression of Eq. (13) becomes

$$L_k = \frac{-m_{k1}}{\sqrt{2ar(\cos\theta + \mu_k\sin\theta)}} \quad \text{where } k = 1,2,3 \tag{20}$$

The equations for establishing the field solutions is the same as that for the elliptical notch except those for L_k and m_{31} which can be simplified as

$$m_{31} = \frac{\frac{\overline{f}i}{2}\left(\overline{\Pi} - \Pi\right) + c_{11}\overline{g}\left(\Psi - \overline{\Psi}\right)}{c_{11}\left(f\overline{g} + \overline{f}g\right)} \tag{21}$$

where

$$\Psi = l_3 - (h_1l_1 + h_2l_2) \quad \text{and} \quad \Pi = l_4 - b_{13}l_2 + c_{11}(h_3l_1 + h_4l_2) \tag{22}$$

5. Energy density concept

For a piezoelectric material containing an elliptical cavity, the surface layer energy criterion is only applicable to the surface of the cavity. The strain energy density criterion is then employed to predict the trajectory of crack propagation or failure path at the interior points near the surface. Similar to the pure mechanical case (Sih, 1991), the energy density function for the electromechanical case in the element $\mathrm{d}V$ of a general three-dimensional system can be written as

$$\frac{\mathrm{d}W}{\mathrm{d}V} = \frac{1}{2}\sigma_{ij}\varepsilon_{ij} + \frac{1}{2}E_iD_i \tag{23}$$

Note that the right-hand terms of Eq. (23) can be obtained from Eqs. (7)–(10) to yield an expression involving $1/r$ energy singularity plus nonsingular terms. Hence, the intensity of the strain energy density field (S) can be expressed as

$$S = r\frac{\mathrm{d}W}{\mathrm{d}V} = r(S_1 + S_2/\sqrt{r} + S_3/r) \tag{24a}$$

where the coefficient S_1, S_2, S_3 are dependent on the material constants, the polar angle θ as well as the remote mechanical and electrical loading, as shown in Fig. 1. If the electric field E_2^{∞} and mechanical stress σ_{22}^{∞} are applied at the remote boundary, as shown in Fig. 1, the total energy density factor S can be expressed as

$$S = \pi a\left(A_{11}\sigma_{22}^{\infty^2} + 2A_{12}\sigma_{22}^{\infty}E_2^{\infty} + A_{22}E_2^{\infty^2}\right) \tag{24b}$$

where the coefficients A_{11}, A_{12} and A_{22} are dependent on the materials constants, and the angle θ of the polar coordinate system at the crack tip. Note that the coefficients for a crack are independent of the radius r at the crack tip. However, for an elliptical cavity or a notch these coefficients are dependent upon the radius r originated at the apex of the elliptical cavity (Sih, 1991). The fundamental parameter in this theory, S, is direction sensitive in the sense that it predicts the direction of crack propagation. This is accomplished by calculating the stationary value of S or $\mathrm{d}W/\mathrm{d}V$, with r being the radial distance measured from the crack front. The minimum S value, i.e., $S_{\min}$, is related to dilatation of material elements and is associated with the creation of a free surface that fracture is expected along the line of crack extension.

For the present two-dimensional problems, the direction of crack propagation can be determined by a single variable θ with different values of r giving the same trend. Hence, the necessary and sufficient conditions for the strain energy density factor S to be minimized are as follows:

$$\frac{\partial S}{\partial \theta} = 0 \quad \text{and} \quad \frac{\partial^2 S}{\partial \theta^2} > 0 \quad \text{at } \theta = \theta_0 \tag{25}$$

The minimum energy density factor, which occurs at the crack initiation direction (θ_0) can be determined from Eq. (25).

5.1. Numerical example

In order to demonstrate the suitability of the energy density theory for solving the problem of piezoelectric failure in the case of exact electric boundary conditions, an elliptic crack embedded in a piezoelectric material, PZT-4, is considered. The following material constants have been obtained by Berlincourt et al. (1964):

$$a_{11} = 8.205 \times 10^{-12}, \quad a_{12} = -3.144 \times 10^{-12}, \quad a_{22} = 7.495 \times 10^{-12}, \quad a_{33} = 19.3 \times 10^{-12} \ (\mathrm{m^2N^{-1}})$$
$$b_{21} = -16.62 \times 10^{-3}, \quad b_{22} = 23.96 \times 10^{-3}, \quad b_{13} = 39.4 \times 10^{-3} \ (\mathrm{m^2C^{-1}})$$
$$c_{11} = 7.66 \times 10^{7}, \quad c_{22} = 9.82 \times 10^{7} \ (\mathrm{V^2N^{-1}}).$$

By solving the characteristic equation of μ_k, the three distinct complex roots can be obtained:

$$\mu_1 = 1.21849\mathrm{i}, \quad \mu_2 = -0.2006087 + 1.069879\mathrm{i}, \quad \mu_3 = 0.2006087 + 1.069879\mathrm{i}$$

Therefore, the corresponding values of λ_k, κ_k can be calculated. For an infinite poled PZT-4 plate, containing a central elliptic cavity, subjected to a remote in-plane electric loading, E_2^∞, and mode I mechanical loading, σ_{22}^∞, as shown in Fig. 1, the load parameters reduce to

$$l_1 = -\frac{a\sigma_{22}^\infty}{2}, \quad l_2 = 0, \quad l_3 = \frac{a}{2}\left(\frac{E_2^\infty + b_{22}\sigma_{22}^\infty}{c_{22}}\right), \quad l_4 = -\frac{\mathrm{i}b}{2}\left(E_2^\infty\right) \tag{26}$$

After substituting all expressions into Eq. (18), γ_e is obtained in terms of E_2^∞, σ_{22}^∞, r and ϕ with $\varepsilon_0 = 8.85 \times 10^{-12}$ $\mathrm{NV^{-2}}$ (permittivity of vacuum). As an illustration, for three different ratios between the applied electric field and the applied stress($\beta = E_2^\infty/\sigma_{22}^\infty$), the normalized surface layer energy, $\gamma_e/\delta\sigma^2\pi a$, is plotted against the angle, ϕ, for several values of α $(= b/a)$, as shown in Fig. 2(a)–(c). It should be noted that the length of the major semi-axis, a, is fixed at $a = 0.01$ m for all calculations. In the case of $\beta = -0.01$, for all values of α, the normalized surface layer energy displays a sharp peak near $\phi = 0°$, which is at a symmetrical location, and this peak moves closer to $\phi = 0°$ as $\alpha(= b/a)$ decreases. Since failure occurs at the location of maximum surface layer energy, the minimum load to failure occurs in the region near $\phi = 0°$. In short, as $\alpha \to 0$, initiation of fracture occurs over a range near $\phi = 0°$, as shown in Fig. 2(a). In Fig. 2(b) and (c), the same failure trend can be seen near $\phi = 0°$ as α decreases. As α increases, the failure location moves away from $\phi = 0°$, e.g., failure will occur at around $\phi = -9°$ for $\alpha = 0.5$, around $\phi = -5°$ for $\alpha = 0.25$, and around $\phi = -3°$ for $\alpha = 0.125$. It can be seen that when an elliptical cavity in a homogeneous solid is subjected to remote loading, the maximum surface layer energy occurs in the surface region in the fourth quadrant, i.e., $-90° \leqslant \phi \leqslant 0°$, of the surface region near the right apex of the cavity. For the same remote loading, no matter in which direction the electric field is applied, increase of loading is allowed when the notch tip becomes more blunt. From Fig. 2(a)–(c), it can be seen that as β increases, the peak value of the normalized surface layer energy for $\alpha = 0.125$ increases considerably, but not for other values of α. This is to say, when α becomes smaller, i.e., the elliptical cavity becomes more like a crack, the effect of the loading ratio, β, on the surface layer energy becomes more significant.

By setting $\alpha = 0.0625$ and varying β, similar results are obtained, as shown in Fig. 3. Note that in the calculations, the stress value is fixed while varying the electric field. Therefore, the loading ratio β varies due to the variation of electric field. As the electric field increases from negative to positive, as shown in Fig. 3, the normalized surface layer energy increases while fracture occurs at the same location. This indicates that a negative electric field impedes cracking and the reverse is true for positive electric field.

Naturally, one would like to know how the crack would extend from the initial failure location on the surface of the elliptical notch. As mentioned above, in order to determine the direction of crack propagation, $\theta = \theta_0$, the stationary values ($S_{\min}$) of the strain energy density for various radius vectors need to be calculated. Thus, for each radius r/a, i.e., in a region a distance from the notch surface as shown in Fig. 1, a curve is generated with respect to the angle θ. The calculated results show that for different radius vectors and directions of the applied electric field, the direction of subsequent fracture is always horizontally outward, i.e., in $\theta = 0$ direction, as shown in Figs. 4(a)–(c) and 5. Note that for each of the curves in Figs. 4 and 5, there are five stationary values that satisfy $\partial S/\partial\theta = 0$, but only three satisfy the condition $\partial^2 S/\partial\theta^2 > 0$. The critical fracture loads should be the minimum value of σ^{cr}, which corresponds to the maximum value of S among the three minimum stationary values. Therefore, only the stationary value at

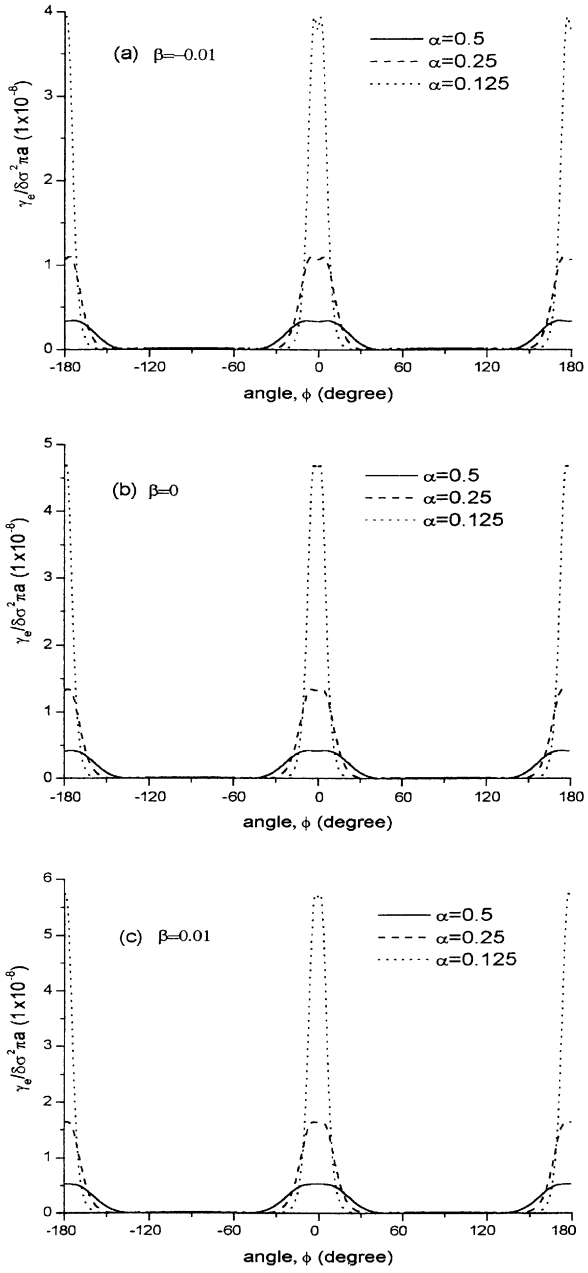

Fig. 2. Variation of the normalized surface layer energy against angle ϕ for different values of α at (a) $\beta = -0.01$; (b) $\beta = 0$; (c) $\beta = 0.01$.

$\theta = 0$ gives the minimum critical fracture load. Thus, the cracking angle should be $\theta_0 = 0$. From Fig. 4(a)–(c), it is obvious that the curve of S versus θ depends not only upon β but also on the value of r. Fig. 5 clearly shows that the normalized S increases with increasing β. Note that the calculated results presented in Figs. 2–5 are obtained based on the assumption that the permittivity of the medium inside the elliptical cavity equals the permittivity of vacuum, i.e., $\varepsilon_0 = 8.85 \times 10^{-12}$ NV^{-2}. Fig. 6 shows the variation of the

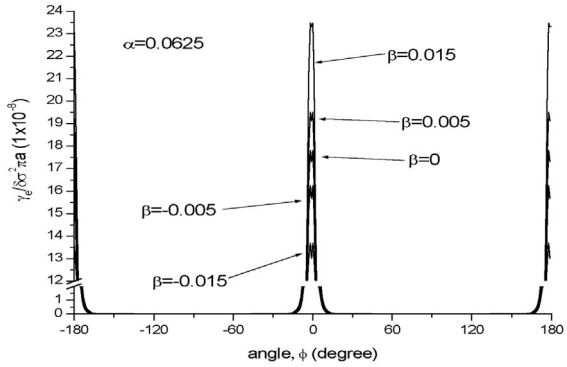

Fig. 3. Variation of the normalized surface layer energy against angle ϕ for different values of β in the case of $\alpha = 0.0625$.

normalized energy density factor against θ for different values of dielectric permittivity of the medium inside the elliptical cavity in the case of $\alpha = 0.000625$ and $r = 0.8 \times 10^{-2}$. The dotted line corresponds to the impermeable condition with $\varepsilon_0 = 0.0\ \mathrm{NV}^{-2}$ and the dashed line represents the permeable condition in which the permittivity of the medium inside the cavity is equal to that of piezoelectric ceramic, i.e. $\varepsilon_0 = 5 \times 10^{-9}\ \mathrm{NV}^{-2}$. The effect of the permittivity of the medium inside the cavity on the energy density factor is obvious.

For fracture analysis of a line crack, which can be regarded as the limiting case of an elliptical cavity, the local energy density can be minimized using Eqs. (24a), (24b) and (25) for prediction of crack propagation when the electric fields are applied in different directions. Without any loss in generality, we choose a fracture stress of 2 MPa obtained when no electric field is applied (Park and Sun, 1995). Note that in the calculations, the condition of $b \to 0$ but $b \neq 0$ (i.e., the crack keeps open) is assumed. It is of interest to examine the effect of the applied electric field on the fracture loads. For the case of exact, impermeable and permeable boundary conditions, i.e., $\varepsilon_0 = 8.85 \times 10^{-12}\ \mathrm{NV}^{-2}$, $\varepsilon_0 = 0.0\ \mathrm{NV}^{-2}$ and $\varepsilon_0 = 5 \times 10^{-9}\ \mathrm{NV}^{-2}$, respectively, the energy density factors for PZT-4 can be expressed as

$$S_{\text{exact}} = 10^{-11}[509.165(E_2^{\infty})^2 + 0.91959(\sigma_{22}^{\infty})^2 + 24.66E_2^{\infty}\sigma_{22}^{\infty}] \tag{27}$$

$$S_{\text{impermeable}} = 10^{-11}[1121.897(E_2^{\infty})^2 + 0.69459(\sigma_{22}^{\infty})^2 + 18.075E_2^{\infty}\sigma_{22}^{\infty}] \tag{28}$$

$$S_{\text{permeable}} = 10^{-11}[509.165(E_2^{\infty})^2 + 2.205787(\sigma_{22}^{\infty})^2 + 16.915E_2^{\infty}\sigma_{22}^{\infty}] \tag{29}$$

Note that these three expressions for S involve both the applied mechanical stress and electric field. The critical fracture stress for a given applied electric field E_2^{∞} can be predicted by substituting S_{cr} $(= A_{11}K_{IC}^2)$ in the above expressions. For easy comparison of the energy density and energy release rate criteria, the energy release rate for an impermeable crack in PZT-4 material is expressed as

$$G = 1 \times 10^{-11}\lfloor 0.036(\sigma_{22}^{\infty})^2 + 0.037\sigma_{22}^{\infty}E_2^{\infty} - 13.8(E_2^{\infty})^2 \rfloor \tag{30}$$

Thus, the fracture stress can also be determined from Eq. (30) for a given applied electric field in terms of the energy release rate. The critical fracture stresses calculated from different fracture criteria and boundary conditions are compared in Fig. 7. The crack propagation is found to be in the x_1 direction for the range of electric field shown in Fig. 7. Moreover, the effect of the direction of the applied electric field on crack propagation for the case of sharp crack is similar to that for the case of elliptical notch, i.e. a negative electric field impedes crack propagation while a positive electric field enhances crack propagation. The critical fracture loads can also be predicted by assuming impermeable crack, i.e., by setting the dielectric

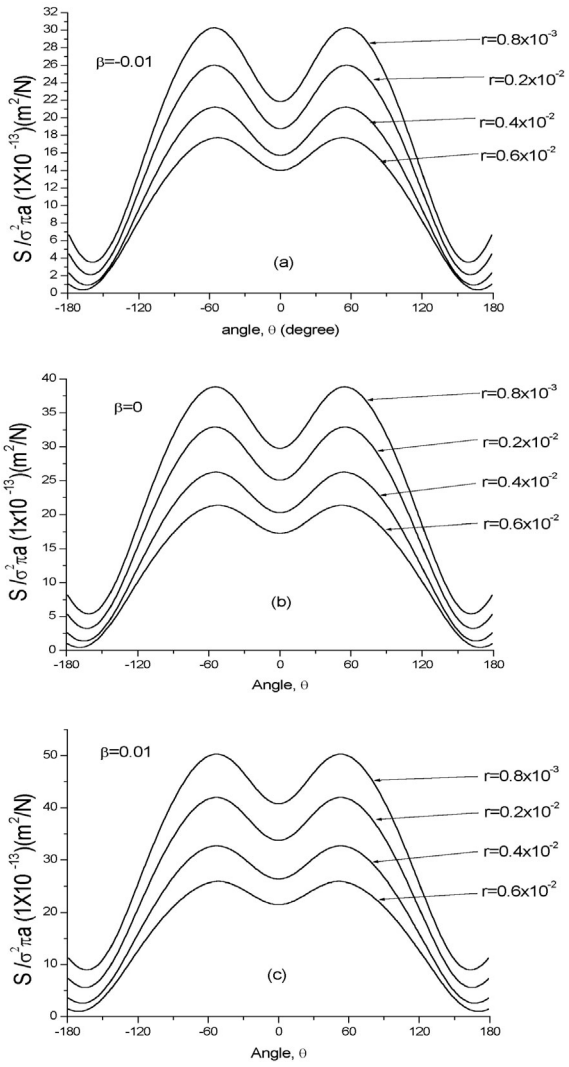

Fig. 4. Variation of the normalized energy density factor against θ for different values of r at (a) $\beta = -0.01$; (b) $\beta = 0$; (c) $\beta = 0.01$.

constant in the cavity, ε_0, to zero. It can be seen from Fig. 7 that the curvature of the curve for the case of impermeable crack is larger than that for the case of exact boundary conditions. This means that the fracture loads are under-estimated by the assumption of impermeable crack (with $\varepsilon_0 = 0.0\ \mathrm{NV}^{-2}$). In other words, the piezoelectric fracture load is under-estimated in the case of impermeable crack subjected to positive applied electric field, i.e., $E_2^{\mathrm{app}} > 0$. However, the curve for the permeable crack (with permittivity equals to that of the piezoelectric ceramic, i.e., $\varepsilon_0 = 5 \times 10^{-9}\ \mathrm{NV}^{-2}$) is above that of the exact boundary condition, indicating that the fracture load is over-estimated by the assumption of permeable crack for $E_2^{\mathrm{app}} > 0$. For the case of $E_2^{\mathrm{app}} < 0$, the trend is reversed for both the impermeable and permeable cracks. In contrast to the energy density criterion, the fracture loads calculated based on the criterion of energy release rate are independent of the direction of the applied electric field (as shown in Fig. 7) which contradicts many experimental observations. The dependence of the fracture loads, calculated from the energy density

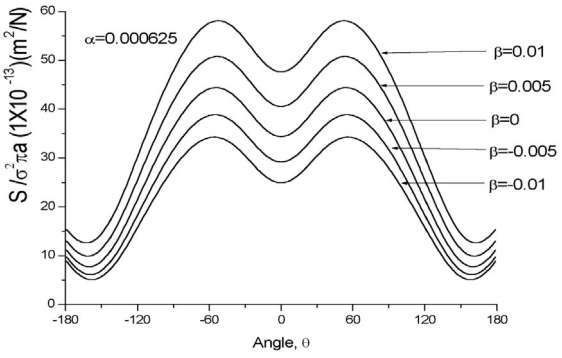

Fig. 5. Variation of the normalized energy density factor against θ for different values of β in the case of $\alpha = 0.000625$ and $r = 0.8 \times 10^{-2}$.

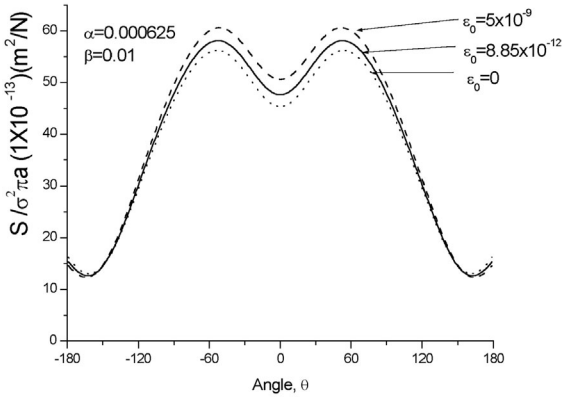

Fig. 6. Variation of the normalized energy density factor against θ for different values of dielectric permittivity of the medium inside the elliptical cavity in the case of $\alpha = 0.000625$ and $r = 0.8 \times 10^{-2}$.

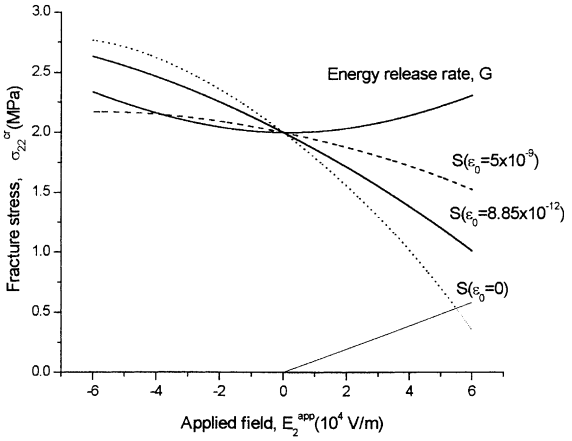

Fig. 7. Effects of the applied electric field on the fracture stress in the case of $\alpha \to 0$.

criterion, on the direction of the applied electric field can be clearly seen in Fig. 7. Note that the four curves intersect at the point of zero applied electric field, which is the case of pure mechanical loading. It is worth mentioning that when the applied electric field, or the loading ratio $\beta(=E/\sigma)$ is out of the region bounded by the straight line that intersect the dotted curve, as shown in Fig. 7, the direction of crack propagation is no longer along the plane $\theta = 0$. In addition, in the calculations the applied electric field should be kept below 10^6 V/m, which is the coercive field of piezoelectric ceramic. This is because a high electric field leads to dielectric breakdown.

6. Conclusions

The objective of this paper is to extend a failure criterion, based on the strain energy density theory, for an elliptical cavity or a line crack embedded in an infinite piezoelectric solid, subjected to a combined in-plane electrical and mechanical loading. This has essentially been accomplished through the consistent application of the strain energy density criterion to a thin layer near the cavity/crack boundary and material element in the interior region of the solid. The total energy density factor (S) depends on the material constants, β, α, polar angle, core region near the apex of the elliptical cavity, and the permittivity of vacuum. The core region on the cavity/crack boundary remains unspecified in size because of different material behavior external to the core region. Unstable crack extension is assumed to occur when some small element just outside the core region has absorbed as much elastic energy as possible and releases it to allow material separation.

As discussed above, the location on the free surface of a cavity, at which the surface layer energy is the maximum, may be postulated to be the location where initial failure occurs. Subsequently, the immediate post-failure crack direction may be determined by minimizing the total energy density factor. The results obtained in this paper by introducing the exact electric boundary conditions on the cavity/crack boundary are more realistic because it reflects the practical situation. In short, the superiority of the energy density theory has been clearly shown from its capability of adopting the exact boundary conditions. For example, the calculated results show that the fracture loads are under-estimated by the assumption of impermeable crack and over-estimated by the assumption of permeable crack for $E_2^{\text{app}} > 0$.

Acknowledgements

Support from the Research Grants Council of the Hong Kong Special Administrative Region, China (Project no. *HKU 7122/99E*), from the Croucher Foundation Chinese Visitorship, and from the National Science Foundation of China under grants #19891180 and #59772017 is acknowledged.

References

Berlincourt, D.A., Curran, D.R., Jaffe, H., 1964. Piezoelectric and piezoceramic materials and their function in transducers. Physical Acoustics, vol. I-A. Academic Press, New York.

Deeg, W.F., 1980. The analysis of dislocation, crack and inclusion problems in piezoelectric solids. Ph.D. Thesis, Stanford University.

Dunn, M.L., 1994. The effect of crack face boundary conditions on the fracture mechanics. Engng. Fract. Mech. 48, 25–39.

Fang, D.N., Liu, B., Hwang, K.C., 2000. Energy analysis on fracture of ferroelectric ceramics. Int. J. Fract. 100 (4), 401–408.

Fang, D.N., Soh, A.K., 2001. Finite element modeling of electromechanical coupled analysis for ferroelectric ceramic materials with defects. Comput. Meth. Appl. Mech. Engng, 190 (22–23), 2771–2787.

Gao, H., Zhang, T.Y., Tong, P., 1997. Local and global energy release rates for an electrically yielded crack in a piezoelectric ceramic. J. Mech. Phys. Solids 45, 491–510.

McMeeking, R.M., 1989. Electrostrictive forces near crack-like flaws. J. Appl. Math. Phys. 40, 615–627.
McMeeking, R.M., 1990. A *J*-integral for the analysis of electrically induced mechanical stress at cracks in elastic dielectrics. Int. J. Engng Sci. 28, 605–613.
Pak, Y.E., 1990. Crack extension force in a piezoelectric material. Trans. ASME, J. Appl. Mech. 57, 647–653.
Park, S., Sun, C.T., 1995. Fracture criteria of piezoelectric ceramic. J. Am. Ceram. Soc. 78, 1475–1480.
Parton, Y.E., 1976. Fracture mechanics of piezoelectric materials. Acta Astronautica 3, 671–683.
Shen, S., Nishioka, T., 2000. Fracture of piezoelectric materials: energy density criterion. Theor. Appl. Fract. Mech. 33, 57–65.
Sih, G.C., 1991. Mechanics of Fracture Initiation and Propagation. Kluwer Academic Publishers, Dordrecht.
Sosa, H.A., Pak, Y.E., 1990. Three-dimensional eigenfunction analysis of a crack in a piezoelectric material. Int. J. Solids Struct. 26, 1–15.
Sosa, H.A., 1992. On the fracture mechanics of piezoelectric soilds. Int. J. Solids Struct. 29, 2613–2622.
Sosa, H.A., Khutoryansky, N., 1996. New developments concerning piezoelectric materials with defects. Int. J. Solids Struct. 33, 3399–3414.
Suo, Z., Kuo, C.M., Barnett, D.M., Willis, J.R., 1992. Fracture mechanics for piezoelectric ceramics. J. Mech. Phys. Solids 40, 739–765.
Zhang, T.Y., Tong, P., 1996. Fracture mechanics for a mode III crack in a piezoelectric material. Int. J. Solids Struct. 33, 343–359.